Simulation of mission with low-thrust spacecraft to near-Earth asteroid

O. L. Starinova[1,2], D. Chen[2], E. Sergaeva[1]

[1]Samara National Research University, Moskovskoe Shosse 34A, Samara, Russia, 443086
[2]Nanjing University of Science and Technology, China

Abstract. In recent years, the study of the small celestial bodies with stable Earth orbits is recognized as an urgent problem by scientists around the world. This is due to the relatively easy availability of such bodies and the ability to obtain important scientific results using the small spacecraft or even the nano-class spacecraft. The use of electric propulsion will further reduce the cost of such missions. However, at present, no methods have been developed for the formation of the control programs and the spacecraft trajectories for such missions. This article is devoted to solving this problem. We obtained the optimal duration control program for the flight to the asteroid 2016NO3 based on the averaged equations of the spacecraft motion. We solved the simulation and the mission design problems for several different variants of the spacecraft design parameters.

1. Introduction

Over the past decade, there has been a significant increase in interest in the study of asteroids, comets and small satellite planets. This is due to the shifting of the research vector toward the solution of applied problems: counteraction to asteroid and comet hazard [1] and development of small solar system objects with the purpose of extraction of minerals [2].

When designing research missions, there is a problem of the development of spacecraft control schemes in the fields of bodies attraction with complex geometric shapes. The gravitational force between the elementary masses in such bodies is not sufficient to form the bodies near-correct geometric shape (ellipsoidal and spheroidal surface). Complex geometry produces the gravitational field of the complex configuration. The spacecraft's behaviour in this field is significantly different from behaviour of spacecraft near ellipsoidal and spheroidal bodies, the shape of which, as well as the gravitational field, may be considered correct in some approximation. The spacecraft motion modelling and the development of control schemes near asteroids and comets are possible only under the condition that the task of these bodies gravitational field formalization was solved with the prescribed accuracy. If however to take into consideration the centre of masses displacement, cavities and voids in the object structure, and the uneven distribution of density [3], it becomes difficult to solve the problem of these objects gravitational field formalization. Since the overloaded model of gravitational potential makes the task of the spacecraft motion modelling and the task of finding optimal sustainable control schemes virtually non-solvable. Thus, the task is to find a balance between the accuracy of the object's potential presentation and the convergence property of the task.

In a number of sources, the problem of finding an accurate mathematical description of the gravitational fields of different objects was addressed. Thus, in the paper [4], the authors address the polygonal method of presenting the gravitational potential of asteroid 4769 Castalia as a formal model.

A comparison takes place of the proposed approach with the model of point attracting centre. In the paper [5], the authors present a comparative analysis of the polygonal model and the model of point attracting centre for the asteroid Cleopatra 216. In the paper [6], the authors present a comparative analysis of the gravitational potential presented in the form of series expanded into spherical, spheroidal, ellipsoidal functions for Martian moons. In the paper [7], the authors address the position of equilibrium points for 23 different asteroids in their polygonal models of gravitational fields.

The drawbacks of the approaches addressed are their cumbersomeness when using in the problems of spacecraft flight dynamics and the necessity to know in advance the physical properties of the objects - geometry and mass distribution. Modelling the gravitational field of objects whose properties and structure are not known in advance within the models described is not possible.

In this paper, the authors provide a comparative analysis of the methods of modelling the gravitational field of the object with a complex geometric shape, using asteroid 2016NO3as an example. This choice is due to the availability of a sufficient amount of studied material on this asteroid [8], [9], [10] that provides a fundamental basis for correlation the modelling results. In addition, the asteroid is massive enough to ignore the uneven distribution of its gravitational field in space [10].

From the demonstration of the developed countries use the technology to systematically target the use of nanosatellites. The main areas of commercial use of the nano-class spacecraft are currently providing communication and retransmission of information for public and commercial consumers, as well as obtaining information from remote sensing of the Earth. For small remote sensing spacecraft, the desire to obtain high-resolution images necessitates the use of low orbits.

The paper analyses the optimal transition between non-planar orbits of a nanosatellite with low-thrust engines. Since the spacecraft has a single engine (taking into account the characteristics of the nano-class spacecraft), the acceleration from the thrust of the engines is constant in magnitude and directed along the binormal or transversal. The purpose of this work is to develop a method for modeling the controlled motion of a spacecraft with low-thrust engines for non-planar flights between low Earth orbit (LEO) and the orbit of a near-Earth asteroid 2016NO3.

2. Mathematical model of controlled motion

Under the action of low thrust, the motion of the apparatus can be described by Newton's equations of the theory of perturbed motion.

$$\frac{dA}{dt}=\frac{2p}{(1+e)^2}\sqrt{\frac{p}{\mu}}\left(e\sin\vartheta a_r+(1+e\cos\vartheta)a_\tau\right), \tag{1}$$

$$\frac{d\lambda_1}{dt}=\sqrt{\frac{p}{\mu}}\left(-\cos u a_r+\left(1+\frac{r}{p}\right)\sin u a_\tau+\frac{r}{p}\left(\lambda_1 a_\tau-\lambda_2 a_n\cot i\ \sin u\right)\right), \tag{2}$$

$$\frac{d\lambda_2}{dt}=\sqrt{\frac{p}{\mu}}\left(\sin u\, a_r+\left(1+\frac{r}{p}\right)\cos u a_\tau+\frac{r}{p}\left(\lambda_2 a_\tau+\lambda_2 a_n\cot i\ \sin u\right)\right), \tag{3}$$

$$\frac{d\Omega}{dt}=\sqrt{\frac{p}{\mu}}\frac{\sin u}{(1+e\cos u\ \sin i)}a_n, \tag{4}$$

$$\frac{di}{dt}=\sqrt{\frac{p}{\mu}}\frac{\cos u}{(1+e\cos u)}a_n, \tag{5}$$

$$\frac{d\tau}{dt}=\frac{p^2}{e\mu(1+e\cos\vartheta)^2}(eN\sin\vartheta-\cos\vartheta)a_r+\frac{N}{1+e\cos\vartheta}a_\tau, \tag{6}$$

where $u=\omega+\vartheta$ is the argument of latitude; $N=\dfrac{2}{1+e\cos\vartheta}\displaystyle\int_0^u\frac{\cos\vartheta'}{(1+e\cos\vartheta')^3}d\vartheta'$; $A=\dfrac{p}{1-e^2}$ is the semimajor axis; $\lambda_1=e\cos\omega$, $\lambda_2=e\sin\omega$ are the components of the Laplace vector; e is the

eccentricity; p is the focal parameter; ω is the argument of periapsis; i is the inclination; τ is the epoch; ϑ is the true anomaly; t is the current time; $\mathbf{a} = \left(a_r, \quad a_\tau, \quad a_n\right)^T$ is the acceleration vector with it's the components in orbital frame.

The long duration of the controlled process and the cyclical changes in the phase coordinates determine the feasibility of the transition to averaged equations. To carry out the averaging procedure, we move from the derivatives of the osculating elements in time to the derivatives of the latitude argument. The system of equations (1) – (6) will take the form:

$$\frac{dA}{dt} = \frac{2A^{9/4}}{\mu} a_\tau \frac{1}{1 - e\cos\vartheta}, \tag{7}$$

$$\frac{d\lambda_1}{dt} = \frac{r^2\gamma}{\mu}\left(-\cos u a_r + \left(1 + \frac{r}{p}\right)\sin u a_\tau + \frac{r}{p}\left(\lambda_1 a_\tau - \lambda_2 a_n \cot i \ \sin u\right)\right), \tag{8}$$

$$\frac{d\lambda_2}{dt} = \frac{r^2\gamma}{\mu}\left(\sin u a_r + \left(1 + \frac{r}{p}\right)\cos u a_\tau + \frac{r}{p}\left(\lambda_2 a_\tau - \lambda_1 a_n \cot i \ \sin u\right)\right), \tag{9}$$

$$\frac{d\Omega}{dt} = \frac{r^3\gamma}{\mu p}\frac{\sin u}{\sin i} a_n, \tag{10}$$

$$\frac{di}{dt} = \frac{r^2\gamma}{\mu}\cos u a_n, \tag{11}$$

$$\frac{d\bar{u}}{dt} = 1 - \frac{r^2\gamma\sqrt{(p)}}{\sqrt{p(r)}}, \tag{12}$$

$$\gamma = \frac{1}{1 - \frac{r^3}{\mu p} a_n \cot i \sin u}. \tag{13}$$

Due to the need to maintain the orientation of the spacecraft relative to the asteroid, the use of thrust directed along the radius vector is difficult and in the future it is assumed that two accelerations are used for control - binormal (perpendicular to the plane of the orbit) and transversal. Using this we get a transformed system of equations (7) – (13) to the systems:

$$\frac{dA}{du} = \frac{2A^3}{\mu} a_\tau, \tag{14}$$

$$\frac{d\lambda_1}{du} = \frac{A^2}{\mu}\left(2\sin u a_\tau + \lambda_1 a_\tau - \lambda_2 a_n \cot i \ \sin u\right), \tag{15}$$

$$\frac{d\lambda_2}{du} = \frac{A^2}{\mu}\left(\cos u a_\tau + \lambda_2 a_\tau - \lambda_1 a_n \cot i \ \sin u\right), \tag{16}$$

$$\frac{d\Omega}{du} = \frac{A^2}{\mu}\frac{\sin u}{\sin i} a_n, \tag{17}$$

$$\frac{di}{du} = \frac{A^2}{\mu}\cos u a_n, \tag{18}$$

$$\frac{d\bar{u}}{du} = \sqrt{\mu}\left(A^{-3/2} - A_k^{-3/2}\right), \tag{19}$$

Here $a_n = \delta_n a_0$ is the binormal acceleration component; $a_\tau = \delta_\tau a_0$ is the transversal acceleration component; $\delta_n \in \{-1, \ 0, \ 1\}$ is the on-off binormal acceleration component function; $\delta_\tau \in \{-1, \ 0, \ 1\}$ is the on-off transversal acceleration component function. Due to energy limitations, only one engine can be switched on at a time, either by binormal or by transversal that is;

$$\left|\delta_n\right| + \left|\delta_\tau\right| \le 1. \tag{20}$$

3. Choosing the method of optimal control

3.1. Controlling structure on the turn

To determine the optimal control structure on the turn, we will solve the problem of the shortest flight duration. In accordance with the maximum principle, it is necessary to select such coordinates of the switching points of the engine u_i that deliver the maximum to the Hamiltonian H:

$$H = \psi_A \frac{2A^3}{\mu} a_\tau + \psi_{\lambda_1} \frac{A^2}{\mu}\left(2\sin u a_\tau + \lambda_1 a_\tau - \lambda_2 a_n \cot i \ \sin u\right) + \psi_{\lambda_2} \frac{A^2}{\mu}\left(\cos u a_\tau + \lambda_2 a_\tau - \right.$$
$$\left. - \lambda_1 a_n \cot i \ \sin u\right) + \psi_\Omega \frac{A^2}{\mu} \frac{\sin u}{\sin i} a_n + \psi_i \frac{A^2}{\mu} \cos u a_n + \psi_{\bar{u}} \sqrt{\mu}\left(A^{-3/2} - A_k^{-3/2}\right). \quad (21)$$

We rewrite the Hamiltonian in the form:

$$H = H_\tau + H_n + H_0 =$$
$$= \delta_\tau a_0 \left(\psi_A \frac{2A^3}{\mu} + \psi_{\lambda_1} \frac{A^2}{\mu}\left(2\sin u + \lambda_1\right) + \psi_{\lambda_2} \frac{A^2}{\mu}\left(2\cos u + \lambda_2\right)\right) +$$
$$+ \delta_n a_0 \left(-\psi_{\lambda_1} \frac{A^2}{\mu} \lambda_2 \cot i \ \sin u - \psi_{\lambda_2} \frac{A^2}{\mu} \lambda_1 \cot i \ \sin u + \psi_\Omega \frac{A^2}{\mu} \frac{\sin u}{\sin i} + \psi_i \frac{A^2}{\mu} \cos u \right) + \quad (22)$$
$$+ \psi_{\bar{u}} \sqrt{\mu}\left(A^{-3/2} - A_k^{-3/2}\right).$$

Since H_0 does not depend on the control, the maximum of the Hamiltonian under the technical restriction (20) is achieved under the following conditions:

$$\begin{cases} \delta_\tau = 1, \ \delta_n = 0, \ \text{если} \ \left(|H_\tau| \geq |H_n|\right) \wedge \left(H_\tau > 0\right) \\ \delta_\tau = -1, \ \delta_n = 0, \ \text{если} \ \left(|H_\tau| \geq |H_n|\right) \wedge \left(H_\tau < 0\right) \\ \delta_\tau = 0, \ \delta_n = 1, \ \text{если} \ \left(|H_\tau| \leq |H_n|\right) \wedge \left(H_n > 0\right) \\ \delta_\tau = 0, \ \delta_n = -1, \ \text{если} \ \left(|H_\tau| \leq |H_n|\right) \wedge \left(H_n < 0\right) \end{cases} \quad (23)$$

The graphs of the functions $H_\tau(u)$ and $H_n(u)$ are sinusoids with the same period (Fig. 2). Therefore, to ensure the maximum of the Hamiltonian, there must be no more than four engine switching points on the turn. For example, for a certain point in time for the values $H_\tau(u)$ and $H_n(u)$ shown in Figure 2, the control structure on the turn will have the form as shown in figure 3.

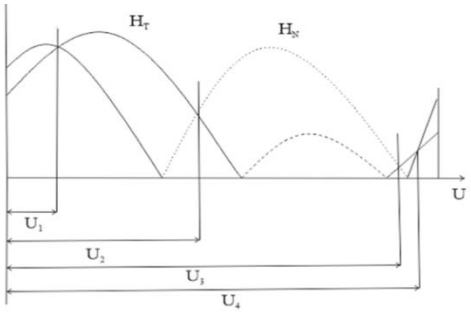

Figure 2. Schematic representation of engine switching points to the $H_\tau(u)$ and $H_n(u)$.

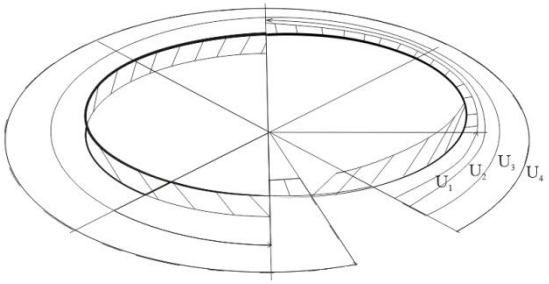

Figure 3. Control structure on a turn, corresponding to the figure 2.

3.2. Averaged equations of motion

For an optimal control structure on the turn (23), we average the equations (14) – (19) over a time interval equal to one period of the satellite's rotation. Denoting by $[A]$, $[\lambda_1]$, $[\lambda_2]$, $[\Omega]$, $[i]$, $[\bar{u}]$ the

averaged values of the derivatives $\frac{dA}{du}$, $\frac{d\lambda_1}{du}$, $\frac{d\lambda_2}{du}$, $\frac{d\Omega}{du}$, $\frac{di}{du}$, $\frac{d\bar{u}}{du}$, we have $[A]=\frac{1}{2\pi}\int_0^{2\pi}\frac{dA}{du}du$.

After performing the integration, and denoting u_1, u_2, u_3, u_4 are the arguments of the latitude of the engine switching points and going to the slow-time t as the new variable, the averaged equations will have the form:

$$\frac{dA}{dt}=\frac{2A^{3/2}}{\pi\mu}a_0\left(u_2-u_1+2\pi+u_3-u_4\right), \tag{24}$$

$$\frac{d\lambda_1}{dt}=\frac{A^{1/2}}{\pi\sqrt{\mu}}a_0\left(\cos u_1-\cos u_2+\cos u_4-\cos u_3\right), \tag{25}$$

$$\frac{d\lambda_2}{dt}=\frac{A^{1/2}}{\pi\sqrt{\mu}}a_0\left(\sin u_2-\sin u_1+\sin u_3-\sin u_4\right), \tag{26}$$

$$\frac{d\Omega}{dt}=\frac{A^{1/2}}{2\pi\sqrt{\mu}\sin i}a_0\left(-\cos u_3+\cos u_2+\cos u_1-\cos u_4\right), \tag{27}$$

$$\frac{di}{dt}=\frac{A^{1/2}}{2\pi\sqrt{\mu}}a_0\left(\sin u_3-\sin u_2-\sin u_1+\sin u_4\right), \tag{28}$$

$$\frac{d\bar{u}}{dt}=\sqrt{\mu}\left(A^{-3/2}-A_k^{-3/2}\right). \tag{29}$$

When constructing algorithms for controlling the spacecraft motion with a low thrust, it is necessary to take into account that even small perturbing forces lead to significant deviations of the device from the calculated trajectory. It is known that the influence of the non-spherical Earth gravity field of is mainly described by the second term of the expansion of the gravitational field potential in the spherical functions. Therefore the long changes in the orbital elements due to the influence of corrective acceleration and the influence of the off center gravity field of the Earth can be described by the following system of equations:

$$\frac{dA}{dt}=\frac{2A^{3/2}}{\pi\mu}a_0\left(u_2-u_1+2\pi+u_3-u_4\right), \tag{24}$$

$$\frac{d\lambda_1}{dt}=\frac{A^{1/2}}{\pi\sqrt{\mu}}a_0\left(\cos u_1-\cos u_2+\cos u_4-\cos u_3\right)+\frac{\varepsilon\left(4-5\sin^2 i\right)}{2\sqrt{\mu}A^{7/2}}\lambda_2, \tag{25}$$

$$\frac{d\lambda_2}{dt}=\frac{A^{1/2}}{\pi\sqrt{\mu}}a_0\left(\sin u_2-\sin u_1+\sin u_3-\sin u_4\right)-\frac{\varepsilon\left(4-5\sin^2 i\right)}{2\sqrt{\mu}A^{7/2}}\lambda_1, \tag{26}$$

$$\frac{d\Omega}{dt}=\frac{A^{1/2}}{2\pi\sqrt{\mu}\sin i}a_0\left(-\cos u_3+\cos u_2+\cos u_1-\cos u_4\right)-\frac{\varepsilon\cos i}{\sqrt{\mu}A^{7/2}}, \tag{27}$$

$$\frac{di}{dt}=\frac{A^{1/2}}{2\pi\sqrt{\mu}}a_0\left(\sin u_3-\sin u_2-\sin u_1+\sin u_4\right). \tag{28}$$

Here $\varepsilon=2,634\cdot10^{10}$ km^5/s^2.

3.3. The solution of time-optimal tasks on the orbital transfer

Let's write the boundary conditions as:

$$\begin{cases}t=t_0,\ \mathbf{x}(t_0)=\mathbf{x}_0,\\ t=t_1,\ \mathbf{x}(t_1)=\mathbf{x}_1,\end{cases} \tag{29}$$

Where $\mathbf{x}=\left(A,\ \lambda_1,\ \lambda_2,\ \Omega,\ i,\ \bar{u}\right)^T$ is the state vector. We formulate a variational time-optimal problem about the interorbital transfer: it is necessary to choice the controlled functions $u_i(t)$ which

provide the transfer of the state point from the position $\mathbf{x}_0$ to the position $\mathbf{x}_1$ in the minimum time under the differential equations of motion (24) – (28) and boundary conditions (29). The acceleration value a_0 is considered to be set.

Let's solve the problem using the Pontryagin maximum principle. Let us introduce the co-state vector $\boldsymbol{\psi} = \left(\psi_A, \quad \psi_{\lambda_1}, \quad \psi_{\lambda_2}, \quad \psi_\Omega, \quad \psi_i, \quad \psi_{\bar{u}}\right)^T$ and construct the Hamiltonian:

$$\begin{aligned} H = {} & \psi_A \frac{2A^{3/2}}{\pi\mu} a_0 \left(u_2 - u_1 + 2\pi + u_3 - u_4\right) + \\ & + \psi_{\lambda_1} \left(\frac{A^{1/2}}{\pi\sqrt{\mu}} a_0 \left(\cos u_1 - \cos u_2 + \cos u_4 - \cos u_3\right) + \frac{\varepsilon\left(4 - 5\sin^2 i\right)}{2\sqrt{\mu} A^{7/2}} \lambda_2 \right) + \\ & + \psi_{\lambda_2} \left(\frac{A^{1/2}}{\pi\sqrt{\mu}} a_0 \left(\sin u_2 - \sin u_1 + \sin u_3 - \sin u_4\right) - \frac{\varepsilon\left(4 - 5\sin^2 i\right)}{2\sqrt{\mu} A^{7/2}} \lambda_1 \right) + \\ & + \psi_\Omega \left(\frac{A^{1/2}}{2\pi\sqrt{\mu}\sin i} a_0 \left(-\cos u_3 + \cos u_2 + \cos u_1 - \cos u_4\right) - \frac{\varepsilon\cos i}{\sqrt{\mu} A^{7/2}} \right) + \\ & + \psi_i \frac{A^{1/2}}{2\pi\sqrt{\mu}} a_0 \left(\sin u_3 - \sin u_2 - \sin u_1 + \sin u_4\right) + \psi_{\bar{u}} \sqrt{\mu} \left(A^{-3/2} - A_k^{-3/2}\right). \end{aligned} \tag{30}$$

From the Hamilton maximum condition we find:

$$\begin{cases} \sin\left(u_1 + \psi_1\right) = -\dfrac{a}{\sqrt{b_1^2 + c_1^2}}, \\ \cos\left(u_1 + \psi_1\right) > 0, \end{cases} \tag{31}$$

$$\begin{cases} \sin\left(u_3 + \psi_1\right) = -\dfrac{a}{\sqrt{b_1^2 + c_1^2}}, \\ \cos\left(u_3 + \psi_1\right) < 0, \end{cases} \tag{32}$$

$$\begin{cases} \sin\left(u_2 + \psi_2\right) = -\dfrac{a}{\sqrt{b_2^2 + c_2^2}}, \\ \cos\left(u_2 + \psi_2\right) > 0, \end{cases} \tag{33}$$

$$\begin{cases} \sin\left(u_4 + \psi_2\right) = -\dfrac{a}{\sqrt{b_2^2 + c_2^2}}, \\ \cos\left(u_4 + \psi_2\right) < 0, \end{cases} \tag{34}$$

Here $\cos\psi_1 = -\dfrac{b_1}{\sqrt{b_1^2 + c_1^2}}$, $\sin\psi_1 = -\dfrac{c_1}{\sqrt{b_1^2 + c_1^2}}$; $\cos\psi_2 = -\dfrac{b_2}{\sqrt{b_2^2 + c_2^2}}$; $\sin\psi_2 = -\dfrac{c_2}{\sqrt{b_2^2 + c_2^2}}$; $a = \psi_A A a_0$

$b_1 = \psi_{\lambda_1} a_0 + \psi_\Omega \dfrac{a_0}{2\sin i}$; $b_2 = \psi_{\lambda_2} a_0 + \psi_\Omega \dfrac{a_0}{2\sin i}$; $c_1 = \psi_{\lambda_1} a_0 + \psi_i \dfrac{a_0}{2}$; $c_2 = \psi_{\lambda_2} a_0 + \psi_i \dfrac{a_0}{2}$.

Let's write a co-state system:

$$\begin{aligned} \frac{d\psi_A}{dt} = {} & -\frac{3}{2}\psi_A \frac{2A^{1/2} a_0}{\pi\sqrt{\mu}} \left(u_2 - u_1 + 2\pi + u_3 - u_4\right) - \frac{1}{2} \frac{\psi_{\lambda_1} a_0}{\pi\sqrt{\mu} A^{1/2}} \left(\cos u_1 - \cos u_2 + \cos u_4 - \cos u_3\right) + \\ & + \frac{7}{2} \frac{\psi_{\lambda_1} \varepsilon\left(4 - 5\sin^2 i\right)}{\pi\sqrt{\mu} A^{9/2}} \lambda_2 - \frac{1}{2} \frac{\psi_{\lambda_1} a_0}{\pi\sqrt{\mu} A^{1/2}} \left(\sin u_2 - \sin u_1 + \sin u_3 - \sin u_4\right) - \frac{7}{2} \frac{\psi_{\lambda_2} \varepsilon\left(4 - 5\sin^2 i\right)}{\pi\sqrt{\mu} A^{9/2}} \lambda_1 + \\ & + \frac{3}{2} \psi_{\bar{u}} \sqrt{\mu} A^{-5/2} - \frac{1}{2} \frac{\psi_\Omega a_0}{\pi\sqrt{\mu} A^{1/2}} \left(\sin u_3 - \sin u_2 - \sin u_1 + \sin u_4\right), \end{aligned} \tag{35}$$

$$\frac{d\psi_{\lambda_1}}{dt} = \psi_{\lambda_1} \frac{\varepsilon\left(4-5\sin^2 i\right)}{2\sqrt{\mu}A^{7/2}}, \tag{36}$$

$$\frac{d\psi_{\lambda_2}}{dt} = \psi_{\lambda_2} \frac{\varepsilon\left(4-5\sin^2 i\right)}{2\sqrt{\mu}A^{7/2}}, \tag{37}$$

$$\frac{d\psi_{\bar{u}}}{dt} = 0, \tag{38}$$

$$\frac{d\psi_{\Omega}}{dt} = 0, \tag{39}$$

$$\frac{d\psi_i}{dt} = \frac{5}{2}\frac{\varepsilon\sin 2i}{\sqrt{\mu}A^{7/2}}\left(\psi_{\lambda_1}\lambda_1 - \psi_{\lambda_2}\lambda_2\right) + \psi_{\Omega}\frac{A^{1/2}a_0\cos i}{2\pi\sqrt{\mu}\sin^2 i}\left(-\cos u_3 + \cos u_2 + \cos u_1 - \cos u_4\right) - \\ -\psi_{\Omega}\frac{\varepsilon\sin i}{\sqrt{\mu}A^{7/2}}, \tag{40}$$

4. Conclusion

The paper analysed the optimal transfer between non-planar orbits of a nanosatellite with low-thrust engines. Since the spacecraft has a single engine (taking into account the characteristics of the nano-class spacecraft), the acceleration from the thrust of the engines is constant in magnitude and directed along the binormal or transversal. The purpose of this work is to develop a method to choosing and modeling the controlled motion of a spacecraft with low-thrust engines for non-planar flights between low Earth orbit (LEO) and the orbit of a near-Earth asteroid 2016NO3.

5. Acknowledgments

This research was performed under the RFBR Grant № 20-08-00779_a.

References

[1] Chapman, C.R. On the Earth by asteroids and comet: assessing the hazard / C.R. Chapman, D. Morrison // Nature. – 1994. – Vol. 367(6458). – P. 33-40.
[2] Ross, S.D. Near-Earth asteroid mining space – Pasadena, CA, 2001.
[3] Britt, D.T. Asteroid density, porosity, and structure // Asteroids III, 1987.
[4] Geissler, P. Erosion and ejecta reaccretion on 243 Ida and its moon / P. Geissler, J.-M. Petit, D. Durda, R. Greenberg, W. Bottke, M. Nolan, J. Moore // Icarus. – 1996. – Vol. 120. – P. 140.
[5] Ren, Y. On tethered sample and mooring systems near irregular asteroids / Y. Ren, J. Shan // Advances in Space Research. – 2014. – Vol. 54(8). – P. 1608-1618.
[6] Hu, X. A numerical comparison of spherical, spheroidal and ellipsoidal harmonic gravitational field models for small non-spherical bodies: examples for the Martian moons / X. Hu, C. Jekeli // Journal of Geodesy. – 2015. – Vol. 89(2). – P. 159-177.
[7] Wang, X. Analysis of the potential field and equilibrium points of irregular-shaped minor celestial bodies / X. Wang, Y. Jiang, S. Gong //Astrophysics and Space Science. – 2014. – Vol. 353(1). – P. 105-121.
[8] Michel, P. The orbital evolution of the asteroid Eros and implications for collision with the Earth / P. Michel, P. Farinella, C. Froeschlé // Nature. – 1996. – Vol. 380(6576). – P. 689.
[9] Garmier, R. Modeling of the Eros gravity field as is ellipsoidal harmonic expansion from the near Doppler track data//Geophysical Research Letters. – 2002. – Vol. 29(8).
[10] Miller, J. K. Determination of shape, gravity, and rotational state of asteroid 433 Eros // Icarus. – 2002. – Vol. 155(1). – P. 3-17.